NIH Public Access
Author Manuscript
Dev Neurobiol. Author manuscript; available in PMC 2014 April 01.

Published in final edited form as:
Dev Neurobiol. 2013 April ; 73(4): 297–314. doi:10.1002/dneu.22060.

Organization of Myelin in the Mouse Somatosensory Barrel Cortex and the Effects of Sensory Deprivation

Kyrstle Barrera[1,2], **Philip Chu**[2,3], **Jason Abramowitz**[2], **Robert Steger**[3], **Raddy L. Ramos**[2,4], and **Joshua C. Brumberg**[2,3]

[1]Department of Psychology, Loma Linda University, Loma Linda, California 92350

[2]Department of Psychology, Queens College, City University of New York, Flushing, New York 11367

[3]Neuropsychology PhD Subprogram, The Graduate Center, City University of New York, New York, New York 10016

[4]Department of Neuroscience and Histology, New York College of Osteopathic Medicine, Old Westbury, New York 11568

Abstract

In rodents, the barrel cortex is a specialized area within the somatosensory cortex that processes signals from the mystacial whiskers. We investigated the normal development of myelination in the barrel cortex of mice, as well as the effects of sensory deprivation on this pattern. Deprivation was achieved by trimming the whiskers on one side of the face every other day from birth. In control mice, myelin was not present until postnatal day 14 and did not show prominence until postnatal day 30; adult levels of myelination were reached by the end of the second postnatal month. Unbiased stereology was used to estimate axon density in the interbarrel septal region and barrel walls as well as the barrel centers. Myelin was significantly more concentrated in the interbarrel septa/barrel walls than in the barrel centers in both control and sensory-deprived conditions. Sensory deprivation did not impact the onset of myelination but resulted in a significant decrease in myelinated axons in the barrel region and decreased the amount of myelin ensheathing each axon. Visualization of the oligodendrocyte nuclear marker Olig2 revealed a similar pattern of myelin as seen using histochemistry, but with no significant changes in Olig2+ nuclei following sensory deprivation. Consistent with the anatomical results showing less myelination, local field potentials revealed slower rise times following trimming. Our results suggest that myelination develops relatively late and can be influenced by sensory experience.

Keywords

myelin; barrel cortex; activity dependent; whiskers; sensory deprivation

INTRODUCTION

Since the initial description of the posteromedial barrel subfield (e.g., barrel cortex) by Woolsey and Van der Loos in 1970, its development, circuitry, thalamocortical connections, and plasticity in response to sensory deprivation have been described in detail (Feldman and

© 2012 Wiley Periodicals, Inc.

Correspondence to: J.C. Brumberg (joshua.brumberg@qc.cuny.edu)..

Kyrstle Barrera and Philip Chu contributed equally to this work.

NIH-PA Author Manuscript
NIH-PA Author Manuscript
NIH-PA Author Manuscript

NIH-PA Author Manuscript

NIH-PA Author Manuscript

NIH-PA Author Manuscript

Brecht, 2005). Mice and rats rely on their whiskers as their primary means of encoding information about the environment. The neurons of the thalamocortical input layer, layer 4, of the primary somatosensory cortex form distinct cytoarchitectonic units known as "barrels." Each barrel corresponds, in a one-to-one fashion, with a specific whisker on the contralateral side of the animal's snout (Woolsey and Van der Loos, 1970). Within layer 4, each barrel is characterized by a cell dense "wall" that surrounds a cell sparse "hollow." Individual barrels are separated by cell-sparse interbarrel regions, called "septa" (Woolsey and Van der Loos, 1970).

The barrel cortex is clearly visible in histological preparations by postnatal day 4 (P4). Sensory deprivation induced by lesions to the whisker follicles within the first few days after birth prevents the formation of the corresponding barrels, whereas lesions after P4 do not impact barrel formation (Durham and Woolsey, 1984; Simons et al., 1984). This is not to say, however, that the barrel field is completely immutable after P4. The barrels continue to be malleable throughout life due to sensory experience, but on a much finer structural and functional scale such as changes in extracellular matrix proteins (McRae et al., 2007), intracolumnar connections (Allen et al., 2003), and thalamocortical projections (Wimmer et al., 2010). These data, taken together, provide evidence for experience-dependent plasticity in the somatosensory cortex long after the critical period for barrel formation has ended.

Following the establishment of mature thalamocortical connections during the second postnatal week, oligodendrocytes begin to myelinate these axons (Wells and Dittmer, 1967; Norton and Poduslo, 1973; Hartman et al., 1982). It has been suggested that the electrical activity of axons plays a role in directing myelinogenesis (Demerens et al., 1996; Mangin et al., 2012). Decreases in the latency of thalamocortical inputs have been observed and are correlated with the late onset of myelination (Shoykhet and Simons, 2008). A consequence of myelination is that the latencies of thalamic inputs decrease their variance and become remarkably consistent (Salami et al., 2003), which are critical for the proper activation of barrel circuit neurons (Pinto et al., 2000; Pesavento et al., 2010). We aimed to characterize the normal development of myelin in the barrel cortex and the impact of sensory deprivation to better understand the role that sensory experience has on structural development within the neocortex.

MATERIALS AND METHODS

Animals

CD1 mice of both sexes were purchased from Charles River Laboratories and then bred in the laboratory. A total of 100 animals were utilized with 37 animals of each sex assigned to the control condition and 63 animals of each sex assigned to the sensory-deprived experimental conditions (Tables 1 and 3). An additional cohort of eight animals was utilized for immunohistochemical studies focusing on myelin basic protein (MBP) expression. Animals were housed together in standard plastic cages with woodchip bedding and *ad libitum* access to food and water. Pregnant females were monitored daily so that the whiskers of the newborn litters could be trimmed within the first 24 h after birth, which we defined as postnatal day 1 (P1). All procedures were approved by the Queens College, CUNY, Institutional Animal Care and Use Committee in accordance with National Institutes of Health guidelines for the responsible use of animals in research.

Sensory Deprivation via Whisker Trimming

For the experimental unilateral trim groups, whiskers on the left side of the animal's face were manually trimmed by holding the animals in the experimenter's hand. Microsurgical spring scissors were used under a 103 magnifying glass. Initial trimming began within the

NIH-PA Author Manuscript

NIH-PA Author Manuscript

NIH-PA Author Manuscript

first 24 h after birth and were trimmed every other day thereafter, ending at P14, P21, P30, P45, P60, or P90. Animals in the "Trim 30-Regrow 30" group were trimmed every other day for the first 30 days, as described, and then the whiskers were allowed to regrow for another 30 days. "Adult Trim 30-60" animals began trimming at P30 and were trimmed every other day for 30 days. "Adult Trim 60-90" animals began trimming at P60 and were trimmed every other day for 30 days. Once animals reached P20, they were anesthetized before trimming to prevent movement and spontaneous whisking. Isoflurane (Aerrane) was delivered using a precision vaporizer for ~5 min at 1–5% before they were trimmed and then allowed to completely awaken before being returned to the cage with their mother. For the age-matched control groups, animal cages were marked with the birth date of the litter and were handled identical to the experimental groups but did not have their whiskers trimmed.

General Tissue Collection and Preparation

At the appropriate developmental age (P14, P21, P30, P45, P60, or P90), animals were anesthetized with an injection of 1.5 mL Euthasol (sodium pentobarbital, Virbac Animal Health) intraperitoneally. Once mice were unresponsive to a noxious stimulus (toe pinch), all animals were perfused transcardially with 0.1 *M* phosphate-buffered saline (PBS) followed by 4% phosphate-buffered paraformaldehyde in 0.1 *M* PBS. Brains were removed from the skull and incubated in 4% phosphate-buffered paraformaldehyde for ~1 h before being washed in PBS. Brains were then cut midsagitally, and the brain stem and midbrain of both hemispheres were removed using a scalpel and fine tweezers. The right hemisphere (contralateral to side of sensory deprivation) was used for each deprived animal as well as each control animal; the left hemispheres were not used for analysis. The cortices were flattened between two glass slides and left in 4% paraformaldehyde for 4–5 days. After the cortices were fixed in the flat position, they were removed from between the slides and kept in 4% paraformaldehyde until they were cut. Cortices were glued to a stage and cut parallel to the pial surface at 50 μm using a vibratome (Ted Pella). They were kept in PBS until they were prepared for staining.

Gold Chloride Myelin Histochemistry

The free-floating slices of cortex were initially incubated in a hydrogen peroxide solution (3 mL of PBS with 60 μL of 30% hydrogen peroxide and 30 μL of 100% methanol) for 20 min on an orbital shaker to decrease background staining due to endogenous peroxidases (e.g., red blood cells). The tissue was then washed three times in 0.01 *M* PBS for 10 min each (3 × 10 min 0.01 *M* PBS) on an orbital shaker and kept in PBS until it was stained.

Sections were stained for myelin as previously published by Wahlsten et al. (2003). To intensify the stain for myelin, we used a 3,3′-diaminobenzidine tetrahydrochloride (DAB) solution (McNally and Peters, 1998). To do so, 5 μg of DAB was dissolved in 5 mL of PBS and then filtered using a 5-mL syringe and a syringe filter unit. The slices of cortex were placed into the solution and 20 μL of 30% hydrogen peroxide was added to catalyze the reaction. The tissue was incubated in this solution for ~5 min and then washed in 5 mL of PBS for ~5 min. The tissue was then placed into 0.2% gold chloride (AuCl, Sigma-Aldrich) in PBS and incubated in an oven at 37°C until the myelin was sufficiently stained, based on visual inspection, which was on average between 2.5 and 3 h. The tissue was then washed twice in 2.5% sodium thiosulfate for 10 min each and kept in PBS until they were mounted.

Slices were mounted onto gelatin-covered slides in PBS. The slides were then allowed to air dry for ~3–4 days, dehydrated in an ethanol series, and placed in xylene for 10 min before cover slipping with DPX mounting medium (Fig. 1).

NIH-PA Author Manuscript

NIH-PA Author Manuscript

NIH-PA Author Manuscript

Myelin Basic Protein Immunocytochemistry

To confirm that our AuCl histochemistry was indeed recognizing the myelin sheath, we conducted a series of experiments where we utilized an antibody to MBP at two developmental ages P32 and P62. The dates slightly differed from the AuCl staining because of staffing issues, but it is unlikely that significant changes in myelin density occur more than 2 days. The tissue was initially processed identically to the AuCl sections before staining. All incubation steps other than the primary antibody were conducted on an orbital shaker. For MBP staining, free-floating sections were rinsed (3 × 10 min 0.01 *M* PBS) and then quenched for peroxidase activity in 1% methanol and 2% H_2O_2 for 30 min. Following washes (3 × 10 min 0.01 *M* PBS) with 1% Triton X-100, sections were blocked in 10% normal goat serum (NGS; Vector Labs) and 1% Triton X-100 (Alfa Aesar) in 0.01 *M* PBS for 1 h. Sections were then incubated overnight (~16 h) at 4°C in a solution consisting of the rabbit polyclonal antibody to MBP (Abcam, AB-40390) at a 1:500 dilution in 0.01 *M* PBS and 10% NGS. The next day, sections were incubated for an additional 30 min, rinsed (3 × 10 min 0.01 *M* PBS), and then incubated in the secondary antibody (goat anti-rabbit; 1:200, Abcam, 97049) with 10% NGS for 2 h. Sections were then rinsed three times in 0.01 *M* PBS (10 min each) and introduced to a standard ABC kit (Vector labs, PK-4000) reaction for 2 h. After rinsing (3 × 10 min 0.01 *M* PBS), sections were placed into a DAB solution (Sigma-Aldrich, Sigmafast tablets), and the reaction was catalyzed using H_2O_2. Sections then underwent a final rinse (3 × 10 min 0.01 *M* PBS) were mounted onto gelatin-coated slides, air-dried overnight, dehydrated in an ethanol series, defatted, and subsequently coverslipped using Permount mounting medium.

Oligodendrocyte Immunocytochemistry and Histology

The sliced cortices were initially incubated identical to what that done for myelin staining. Then, to reveal oligodendrocytes, the tissue was immunohistochemically labeled for Olig2+ oligodendrocytes (Lu et al., 2000; Zhou et al., 2000). Briefly, free-floating sections were blocked in 5% NGS and 0.2% Triton X-100 for 2 h on an orbital shaker. Sections were incubated with the primary antibody (rabbit anti-Olig2, 1:1000, Chemicon) in 2.0% NGS and PBS at 4°C overnight. The sections were then placed on an orbital shaker, rinsed (3 × 10 min 0.01 *M* PBS), and then incubated in a biotinylated secondary antibody (goat anti-rabbit, 1:200, Vector Labs) for 2 h at room temperature. Sections were rinsed (3 × 10 min 0.01 *M* PBS) and incubated for 2 h in a 10% Triton X and avidin–horseradish peroxidase solution. Sections were rinsed in PBS and then reacted with 0.05% DAB in the presence of 0.0015% H_2O_2. Sections were mounted in PBS onto gelatin-coated slides and dried overnight.

After the tissue was labeled for Olig2+ oligodendrocytes, it was counterstained for Nissl to elucidate the barrel region. Slides were then dehydrated in an ethanol series, placed in xylene for 10 min, and cover slipped with DPX mounting medium.

Myelin Data Collection and Analysis

All quantification was done using an Olympus BX51 microscope with a motorized stage (Ludl) and a Microfire camera (Optronics). Numerical densities were estimated using the optical fractionator method for both the AuCl and MBP staining. Stereo Investigator software (Microbrightfield) was used to analyze the surface of each section cut tangentially through layer 4 of the barrel cortex. The contours of the barrel field and each barrel hollow were outlined using a 4× objective (0.10 NA). For each section, three to five barrels that could be clearly identified were outlined in this fashion. Transected axons were counted using an oilimmersion 100× objective (1.4 NA). The barrel field was outlined first, and then each barrel hollow was outlined using a different contour label to distinguish the entire barrel field from the barrel hollows (see Fig. 2). In rats, septal neurons derive their receptive field properties from lemniscal afferents (Brumberg et al., 1999; Furuta et al., 2009) and

NIH-PA Author Manuscript

NIH-PA Author Manuscript

NIH-PA Author Manuscript

barrel wall neurons receive direct thalamocortical inputs (Keller et al., 1985) and because mice do not possess clearly defined septa, we compared the densities of myelinated axons between the barrel hollow and the barrel wall/septal region. The barrels were contiguous and chosen such that it appeared that their entire tangential extent was evident in the same section; the net result was that largely the barrels corresponding to the caudal whiskers were analyzed. It is possible that, as a result, we were unable to quantify gradients of development within the barrel field (e.g., anterior vs. posterior barrels). Stereo Investigator was used to superimpose a randomized grid onto the contour of interest. The randomized grid created sampling sites within each contour. Given that the axons appeared to traverse in a plane perpendicular to the pial surface, only transected axons within those sampling sites were quantified. A minimum of eight random sampling sites were analyzed within each contour, with a grid size of 60 μm × 60 μm and a counting frame size of 20 μm × 20 μm [see Fig. 2(A,C)].

Transected axons were counted within each barrel hollow first, and then the interbarrel septal/barrel wall region was analyzed by counting the entire barrel field contour while excluding the nested barrel hollow contours. Only axons that were transected on the surface of the slice were marked. On average, 58 barrel hollow (range of 23–120) and 55 septal/barrel wall (range of 21–106) sampling sites were analyzed for each animal. Stereo Investigator software was used to quantify the number of transected myelinated axons on the surface of each slice. Using these samples, Stereo Investigator provided an estimate of total axon number in the contour area. Given that the axons frequently ran the entire width (*z*-plane) of the section, we only counted axons at one depth which precluded volumetric analysis. These estimates were subsequently used in statistical analyses.

Axonal diameter measurements were also conducted using Neurolucida software on only the AuCl-stained sections. Using the “Quick Measure Line” tool, 10 randomly selected axonal diameter measurements were made along the widest cross-sectional area of the transected myelinated axon in the barrel hollow region and 10 measurements were made within the septal/barrel wall region for each experimental and control group [see Fig. 2(B)]. All measurements were taken in the same fashion using a 100× lens (1.4 NA) with an approximate *xy* resolution of ~0.02 μm.

Oligodendrocyte Data Collection and Analysis

All quantification was done using an Olympus BX51 as discussed above. Olig2+ oligodendrocytes and Nissl-stained cells were counted within each barrel hollow first, and then the interbarrel septal/barrel wall region was analyzed excluding the nested barrel hollow contours. On average, 55 barrel and 68 septal/barrel wall sampling sites were analyzed for each animal. Using these samples, Stereo Investigator provided an estimate of total Olig2+ oligodendrocyte and total cell numbers in the defined contours. These estimates were subsequently used in statistical analyses.

Local Field Potential Recording Methodology

CD-1 mice were sensory deprived until P60 and their whiskers were allowed to regrow for ~2 weeks. Animals were anesthetized through intraperitoneal injection of ketamine/xylazine (153 and 2.23 mg/kg, respectively) until they were unresponsive to a noxious stimulus (foot pinch). Animals were then placed in a small animal stereotaxic apparatus (David Kopf). A scalpel was used to make an ~3 mm by 3 mm window in the skull from bregma to lambda on both sides of the brain to expose the cortex above the whisker representation in the primary somatosensory region (S1).

NIH-PA Author Manuscript

NIH-PA Author Manuscript

NIH-PA Author Manuscript

The barrel field was localized by inserting a tungsten microelectrode (3–4 MΩ, Frederick Haer) perpendicular to the pial surface and manually driven to a depth of ~300 μm. Activity was amplified, digitized, and recorded (A-M systems model 1700 AC amplifier, 1322A Digidata A/D converter, Molecular Devices, Sunnyvale, CA; Axoscope version 8.0, Molecular Devices), whereas whiskers were manually deflected contralateral to the recording location. Robust, unambiguous responses to contralateral whisker deflection were used as confirmation of barrel cortex. This was done on both the control and sensory-deprived hemispheres within each animal.

Local field potentials (LFPs) were recorded in response to deflection of the whisker on the contralateral side of the face using Clampex software (Molecular Devices). Using a picospritzer (Toohey Instruments, Model IIe) pulses of pressurized N_2 gas (~20 PSI) lasting 100 ms were used to deflect the whiskers. One hundred trials were recorded in each hemisphere with a 2.5-s intertrial interval. This was performed twice on each hemisphere of the brain, once with the jet of air pointing directly at the whiskers and once with the jet of air pointing away from the whisker to confirm the stimulus-driven nature of the LFP.

LFP Data Quantification and Analysis

Trace averages of the 100 trials were computed and graphed for analysis using ClampFit software (Clampex version 8.0, Molecular Devices). Cursors were manually placed at the onset and at the peak of the response, and the slope of the onset response was calculated. These slope values were statistically compared using paired *t*-tests.

Statistical Analyses

Statistical analyses were done using SPSS version 17.0 for Mac OSX. The barrel hollow and septa/barrel wall data were analyzed separately, using a one-way, between-subjects ANOVA followed by Bonferroni-adjusted pairwise comparisons (two-tailed *t*-tests); $p < 0.05$ was arbitrarily chosen to reflect statistical significance.

RESULTS

The Normal Development of Myelin in Barrel Cortex

Myelinated axons in the barrel cortex largely run perpendicular to the pial surface; few myelinated axons were seen running in the plane parallel to the pial surface (see Fig. 1). The myelinated axons traversed the septal/barrel wall areas in large clusters and were less clustered in the barrel hollow, as shown previously (Waite, 1977). In control animals it was qualitatively apparent that the myelinated axon density was greater in the septal/barrel wall areas than within the barrel hollow itself. This is consistent with the finding that NG2+ oligodendrocyte precursor cells are found in higher density in the barrel wall/septa (Mangin et al., 2012). We used a nonbiased stereological sampling technique to quantify the number of cross-sectioned axons contained within the barrel/hollow and in the interbarrel septal/barrel wall region (see Materials and Methods section, Fig. 2). As it is not possible to easily differentiate between the interbarrel septum and the barrel walls in mice, we grouped the counts from those regions and compared them to those quantified from the barrel hollows. At low magnification [see Fig. 3(A–F)], the barrel hollow appears darker at all time points before P90; a similar finding was observed in the rat when immunocytochemical means were used to identify myelin (Seelke et al., 2012). The darker appearance does not appear to be due to a higher density of myelin as the barrel wall contains significantly more myelinated axons [Figs. 2(B), 4, and 7], one possibility is that the thalamic innervations of the barrel are such that axons target the bottom of the barrel and the side walls with a relatively sparse hollow, and thus sections taken through the bottom of the barrel will not

NIH-PA Author Manuscript

NIH-PA Author Manuscript

NIH-PA Author Manuscript

have a hollow and appear inverted relative to the other sections (Lu and Lin, 1993; Kichula and Huntley, 2008).

Early in development when there are relatively few myelinated axons (P14 and P21) and the density of myelinated axons was greater in the barrel hollow, but this difference did not reach statistical significance. From P30 on, the septa/barrel wall region tended to have a higher axonal density than in the barrel hollow, reaching statistical significance at P90 [$t(5)= -3.274$, $p < 0.05$].

We quantified axonal density and axonal diameter in both the hollow and septa/wall at six time points (P14, P21, P30, P45, P60, and P90) and conducted one-way, between-subjects ANOVAs on the data (see Figs. 2 and 3). The analyses for development of axonal density in both the barrel hollow and the septa/barrel wall yielded significant results [$F(13,64) = 36.37$, $p < 0.001$, $F(13,64) = 51.02$, $p < 0.001$, respectively]. *Post hoc* pairwise comparisons were analyzed using the Bonferroni correction to control for the number of groups compared. Myelinated axonal density increased over time, with a statistically significant increase seen from P45 to P60 in both the barrel hollow and in the septa/barrel wall (all $p < 0.01$). In sum, little myelin was observed during the first 6 postnatal weeks in either the barrel hollow or the septa/barrel wall regions, and its appearance appeared to occur simultaneously in these two regions (see Tables 1 and 2, and Fig. 3).

To confirm that AuCl staining was providing an effective image of the myelin within the barrel, we also utilized an antibody targeted to MBP, one of the most abundant proteins associated with the myelin sheath. Immunocytochemical staining revealed a barrel-like pattern at low magnification at both P32 [Fig. 4(A)] and P62 [Fig. 4(B)]. High-magnification images at both developmental time points [Fig. 4(C,D)] showed that the majority of the myelinated axons traverse the slice perpendicular to the tangential slicing plane. There were significant differences in myelin density between the barrel wall and hollow at both time points [P32, $p < 0.01$; P62, $p < 0.05$, Fig. 4(E,F)]. Similar to our AuCl staining, increases in apparent myelination within the barrel hollow were detected across the two age groups we sampled (P32 and P62), and significant increases in barrel wall myelination were also observed ($p < 0.01$, Student's *t*-test). Direct comparisons between AuCl and MBP staining revealed similar qualitative patterns of staining [compare Fig. 5(A,C) to Fig. 5(B,D)] and similar quantitative results [Fig. 5(E,F)]. In sum, our findings using an antibody to MBP mirrored those we observed using AuCl, suggesting that the different methods for visualizing myelin can be used interchangeably.

We then sought to determine if the amount of myelin found ensheathing the axons was constant over early development or increased as function of age. We measured axonal diameters and utilized an ANOVA to determine if there were changes in myelinated axonal diameter across time. The analysis in both the barrel hollow and the septa/barrel wall yielded significant developmental differences [$F(13,766) = 14.685$, $p < 0.001$; $F(13,766) = 18.778$, $p < 0.001$, respectively]. To investigate the nature of these results, *post hoc* pairwise comparisons with Bonferroni corrections were conducted. In the barrel hollow, randomly sampled P60 myelinated axons had significantly larger diameters than P14 axons. In the septa/barrel wall, a significant increase in myelinated axonal diameter was seen after P60 ($p < 0.05$, see Tables 3 and 4, Fig. 6), which then decreased by P90.

Sensory Deprivation Impacts Barrel Cortex Myelination

Once the normal development of myelin was better understood, we sought to explore how sensory deprivation may impact the trajectory of myelination in the mouse barrel cortex. To investigate the effects of sensory deprivation, we unilaterally trimmed the facial vibrissae for specified periods of time starting from birth (see Materials and Methods section). A

NIH-PA Author Manuscript

NIH-PA Author Manuscript

NIH-PA Author Manuscript

significant difference in myelinated axonal density was observed between P60 control animals and animals that were sensory-deprived until P60 in the barrel wall/septa ($p < 0.01$), with no corresponding difference in the barrel hollow (Fig. 7). There was little difference in myelination earlier in life, which may be due to the lack of appreciable myelin early in development.

Lastly, we included regrow and adult trim groups to investigate whether the normal pattern of myelination could be reinstated once trimming occurred, as well as whether a critical period existed for sensory deprivation to affect myelination. To explore whether or not the effects of trimming were reversible, a regrow group was included. Regrow animals were trimmed every other day for the first 30 days, as previously described, and then the whiskers were regrown for another 30 days. The myelinated axonal density was significantly reduced in the regrow group in comparison to same aged control and deprived animals in both the barrel hollow and the septa/barrel wall regions (ps < 0.01, Fig. 7). There were also changes in myelin diameter following trimming (Fig. 8); within the barrel hollow there were significant decreases following 60 days of deprivation ($p < 0.01$), but allowing the whiskers to regrow returned the diameters to control dimensions. In the barrel wall/septal region, significant decreases were observed at both P45 and P60 (ps < 0.01), but again allowing the whiskers to regrow regained the normal myelin diameter. In sum, allowing the whiskers to regrow did not result in the reversion to control patterns for myelin density but did for myelinated axonal diameter.

To better investigate the presence of a critical period within which the sensory deprivation affects myelination, we included two additional “regrow” groups. The Adult Trim 30-30 animals began trimming at P30 and were trimmed for 30 days as previously described. The Adult Trim 60-30 animals began trimming at P60 and were trimmed for 30 days, as previously described. In the barrel hollow, a significant decrease was seen in myelinated axonal density in the Adult Trim 30-30 group in comparison to the P60 control group ($p < 0.01$). The Adult Trim 60-90 group (whisker trimming for 30 days began at P60) showed an increase in myelinated axonal density in comparison to the P90 control group ($p < 0.01$). In the barrel wall/septa, a significant decrease was seen in myelinated axonal density in the Trim 30-30 group in comparison to the age-matched P60 control group ($p < 0.01$). In the Trim 60-90 group, a similar trend was seen as that in the barrel hollow, although the analysis did not reach statistical significance. Thus, delaying the onset of sensory deprivation for 30 or 60 days after birth selectively impacts myelinated axonal density, while leaving myelinated axonal diameter unchanged. These data, taken together, suggest that the density of myelinated axons may have a critical period in the barrel, such that deprivation beginning at P30 decreases myelinated axonal density but deprivation beginning at P60 actually increases myelinated axonal density in the barrel hollow.

Sensory Deprivations Impact on Oligodendrocytes

We then sought to determine if there was a decrease in the number of oligodendrocytes as a result of trimming or an overall decrease in the number of cells within the barrel cortex, which would, in turn, require fewer axons. To address these questions, we labeled the oligodendrocyte marker (Olig2), counterstained with nissl, and quantified Olig2+ nuclei and overall cell density (nissl+ nuclei, which include neurons and glia) using the stereological methods described above [Fig. 9(A,B)]. There was no difference in oligodendrocyte density between sensory-deprived and control animals in either the barrel hollow or the barrel wall/septa [$t(11) = 1.21$, $p = 0.25$; $t(11)$ 1.00, $p = 0.34$, respectively; Fig. 9(C)]. We also did not find a difference in the overall sampled density of postsynaptic cells (Nissl labeled) between control and sensory-deprived animals in either the barrel hollow or the barrel wall/septa [$t(11) = -1.27$, $p = 0.23$; $t(11) = -1.06$, $p = 0.314$, respectively; Fig. 9(D)]. Thus, sensory

NIH-PA Author Manuscript

NIH-PA Author Manuscript

NIH-PA Author Manuscript

deprivation did not impact the oligodendrocyte population or the overall number of cells within the barrel.

Local Field Potentials

To assess the functional consequence of fewer myelinated axons reaching the barrel cortex, we recorded LFPs in layer 4 [Fig. 10(A)] from the deprived side (contralateral to trimming) and undeprived side (ipsilateral to trimming) in a subset of trimmed animals ($n = 6$). The principal whisker in all cases was determined by the manual deflection of the whiskers while amplifying the neural signal. Once the principal whisker was determined, an air puffer was placed over the whisker and 100 ms air puffs were delivered once every 2.5 s deflecting the whisker in the ventral direction. Averages of 100 stimulus presentations [Fig. 10(B)] revealed that although responses on the deprived and control sides initiated at the same time ($p = 0.24$) and had similar response amplitudes ($p = 0.66$), the rate of rise of the responses was significantly different. The rate of rise of the response was significantly slower following deprivation [5.03 vs. 2.53 μV/ms, $t(5) = -2.67$, $p = 0.04$], suggesting that perhaps the deprivation-induced myelin decreases played a role in slowing the whisker-evoked response.

DISCUSSION

Our first aim was to describe the normal development of myelination in the mouse posterior medial somatosensory barrel field. We showed that myelinated axons in normally developing CD-1 mice are sparse before P30 and course perpendicular to the pial surface, traverse the septa/barrel wall in large clusters, and display a diffuse arrangement in the barrel hollow. The relatively late maturation of myelin in the barrel is consistent with previous findings that do not observe myelin until at least the third postnatal week (Vincze et al., 2008) and demonstrate that mature levels of lipids at ~P42 (Wells and Dittmer, 1967), although mature oligodendrocytes are present as early as the first postnatal week in the barrel cortex (Toda et al., 2008). The mature myelination pattern is in contrast to what is seen early in development where there was a tendency for myelination to be denser in the barrel hollow region.

Our second aim was to explore the impact of sensory deprivation on the trajectory of myelin development. Sensory deprivation was found to decrease the density of myelinated axons in the barrel hollow and in the barrel wall/septal region. It was further found that sensory deprivation did not only decrease the density of myelinated axons, but those axons that were myelinated appeared to be ensheathed by less myelin in both the hollow and septa. These effects on axon density were not reversed by allowing the animals' whiskers to regrow after a period of deprivation, but the effect on diameter did reverse. Similar to patterns seen in previous studies (reviewed in Feldman and Brecht, 2005) and other cortical areas (Morishita and Hensch, 2008), there was a critical period in which sensory deprivation had a significant impact. Our results demonstrate that sensory deprivation differentially impacts myelinated axonal density in adulthood, with an increase in myelination within the barrel hollow seen in animals that began sensory deprivation at P60, but no impact was seen on myelinated axonal density in the barrel wall/septa.

There are a number of possibilities that could account for the findings presented in this article. First, there could simply be fewer axons that traverse the posterior medial barrel field following sensory deprivation. Second, our results could reflect a reduction in axonal branching as a result of sensory deprivation. Third, it is possible that there was a reduction in post-synaptic cell density resulting in fewer axons, or a decrease in the number of oligodendrocytes which could result in a smaller quantity of myelinated axons, both of which would account for the reduction in myelinated axonal density. Recent work has

NIH-PA Author Manuscript

NIH-PA Author Manuscript

NIH-PA Author Manuscript

shown that following deprivation there is a decrease in the number or complexity of thalamocortical axons projecting to the barrel cortex (Wimmer et al., 2010). Fewer thalamocortical axons would likely result in sparser myelination, which is consistent with our finding that there are fewer myelinated axons. We cannot rule out that there may also be less branching of thalamocortical axons, which is observed in intracortical axons following deprivation (Bruno et al., 2009). It is unlikely that there is a change in the number of postsynaptic cells as our analysis of nissl-stained cell bodies in this study as well as a previous study (McRae et al., 2007) have found that there was no difference in cell number between control and sensory-deprived animals, and the number of thalamic neurons projecting to the barrel cortex is not impacted by deprivation (Keller and Carlson, 1999). Lastly, it is also possible that sensory deprivation reduced oligodendrocyte density. Our immunohistochemistry analysis of oligodendrocyte density revealed that there were no differences in the oligodendrocyte density between control and sensory-deprived animals, which suggests that sensory deprivation is not significantly impacting the oligodendrocyte population. It is possible that a population of non-Olig2-expressing oligodendrocytes is impacted specifically by sensory deprivation. This seems unlikely because the total number of cells (nissl+ nuclei) in the barrel cortex was also unaffected by sensory deprivation. Previously, it has been shown that there is a relationship between neuronal activity and myelination, with neural-derived electrical activity being a key facilitator of myelin sheath formation (Demerens et al., 1996), and thus the decreased myelin diameter observed in the deprivation studies may be reflective of prolonged decreases in sensory-evoked neural activity. Recent findings have demonstrated that the myelin precursor cells receive excitatory thalamic inputs and their distribution is impacted by a peripheral lesion, which in turn could impact myelination, but a more subtle sensory deprivation (dark rearing) had little impact (Mangin et al., 2012); nevertheless, the results suggest a role in afferent activity in shaping subsequent cortical myelination.

Origin of Myelin Staining

We utilized a histochemical technique developed by Wahlsten et al. (2003) that has been shown to label myelin similar to what is seen using antibodies to MBP or transgenic lines that use the MBP promoter as a tag (see Jacobs et al., 2007). Our finding that mostly axons running perpendicular to the cortical plate were labeled and not those axons running in the horizontal plane is consistent with prior studies showing that many local axons are unmyelinated whereas those coming from extrinsic sources are myelinated (reviewed in Thompson and Bannister, 2003). Furthermore, the observation that myelination is largely not observed superficial to layer 4 is consistent with the known myelination patterns of thalamocortical axons (Salami et al., 2003), although we cannot completely rule out that some of the axons are corticocortical in nature, which have also been shown to rearrange following trimming (Bruno et al., 2009). To complement our AuCl staining, we conducted additional studies using antibodies to MBP, which revealed similar staining patterns both quantitatively and qualitatively, a correspondence that has also been previously noted in cerebellar tissue (Soazo and Garcia, 2007). Finally, in tangential sections, the pattern of myelin staining is characterized by a ring-like appearance, which is consistent with the unmyelinated axon being wrapped by its myelin sheath, suggesting that our staining protocol results in accurate reflection of myelin distribution in the barrel cortex.

Developmental Progression

Our results highlight the fact that myelination occurs relatively late compared with other developmental events in the barrel cortex such as map formation [first postnatal week (reviewed in Inan and Crair, 2007)], peak levels of synaptogenesis [second postnatal week (Micheva and Beaulieu, 1996)], and the onset of whisking [second postnatal week (Landers and Philip Zeigler, 2006)]. Interestingly, many components of the extracellular matrix do not

NIH-PA Author Manuscript

NIH-PA Author Manuscript

NIH-PA Author Manuscript

reach their mature state until the second postnatal month as well (Matthews et al., 2002). It is hypothesized that similar to the extracellular matrix, myelin does not reach its adult levels until after the network has established its adult connectivity patterns, signaling the end of the developmental critical period (Pizzorusso et al., 2002), and resulting in a decrease in the latency of sensory-evoked whisker responses (Shoykhet and Simons, 2008). Unlike other morphological (Durham and Woolsey, 1984; Maravall et al., 2004) and physiological (Simons and Land, 1987) variables, whisker trimming that begins at P30 still impacts myelin levels, although recent data suggest that thalamocortical arbors are impacted by sensory deprivation during adulthood (Oberlaender et al., 2012). This suggests that although the developmental critical period is often thought to include just the first few weeks of life, it might be more accurate to consider that there exist multiple critical periods wherein changes in sensory experience early on can dramatically impact map formation (van der Loos and Woolsey, 1973), dendritic and axonal parameters (Zuo et al., 2005; Wimmer et al., 2010), and physiological responses (Simons and Land, 1987; Feldman, 2000; Sun, 2009; Wilbrect et al., 2010), whereas later alterations in sensory experience can impact other variables such as myelination.

Functional Implications

Our results clearly show that following sensory deprivation there are fewer myelinated axons in the barrel cortex, which may affect signals from the sensory periphery. In addition, action potentials from the thalamus to the barrel cortex may arrive in a more temporally dispersed pattern because axonal diameter, path length, and myelination are the key variables determining conduction velocity (Salami et al., 2003; Yamazaki et al., 2010). Our LFP data are consistent with this hypothesis. Given that there are some myelinated axons remaining following deprivation, this population of axons likely accounts for the lack of difference in response latencies, but the slower rise of the response may be a result of inputs continuing to arrive at longer latencies because of their transmittal over slower conducting unmyelinated or less myelinated axons. The net result of decreased myelination is that when whiskers contact textured surfaces, inputs that normally would illicit discrete volleys of excitatory inputs will now result in overlapping volleys of excitatory inputs, making it harder to discriminate high spatial frequency inputs. This finding is consistent with published behavioral results (Carvell and Simons, 1996). Interestingly, similar deficits in processing high-frequency sensory inputs following early deprivation are seen in other sensory modalities. For example, individuals with amblyopia have deficits in the processing of high spatial frequency inputs (Hess et al., 2009). In addition, following an auditory deprivation paradigm, latencies to high-frequency tones were significantly delayed and the delay was not due to differences in conduction velocities in the peripheral nerves (Clopton and Silverman, 1978). Thus, sensory deprivation-induced decreases in myelination may contribute to an animal's inability to discriminate high-frequency inputs in general, because slowed conduction times due to myelin loss will result in temporally overlapping distributions of action potentials, which can lead to difficulty in making discriminations.

Acknowledgments

The authors thank Maribel Rodriguez for her help with quantification and Dr. Carolyn Pytte for comments on the manuscript.

Contract grant sponsor: NINDS NS058758; contract grant number: NS058758.

REFERENCES

Allen CB, Celikel T, Feldmen DE. Long-term depression induced by sensory deprivation during cortical map plasticity in vivo. Nat Neurosci. 2003; 6:291–299. [PubMed: 12577061]

NIH-PA Author Manuscript

NIH-PA Author Manuscript

NIH-PA Author Manuscript

Brumberg JC, Pinto DJ, Simons DJ. Cortical columnar processing in the rat whisker-to-barrel system. J Neurophysiol. 1999; 82:1808–1817. [PubMed: 10515970]

Bruno RM, Hahn TT, Wallace DJ, de Kock CP, Sakmann B. Sensory experience alters specific branches of individual corticocortical axons during development. J Neurosci. 2009; 29:3172–3181. [PubMed: 19279254]

Carvell GE, Simons DJ. Abnormal tactile experience early in life disrupts active touch. J Neurosci. 1996; 16:2750–2757. [PubMed: 8786450]

Clopton BM, Silverman MS. Changes in latency and duration of neural responding following developmental auditory deprivation. Exp Brain Res. 1978; 32:39–47. [PubMed: 207547]

Demerens C, Stankoff B, Logak M, Anglade P, Allinquant B, Couraud F, Zalc B, et al. Induction of myelination in the central nervous system by electrical activity. Proc Natl Acad Sci USA. 1996; 93:9887–9892. [PubMed: 8790426]

Durham D, Woolsey TA. Effects of neonatal whisker lesions on mouse central trigeminal pathways. J Comp Neurol. 1984; 223:424–447. [PubMed: 6707253]

Feldman DE. Timing-based LTP and LTD at vertical inputs to layer II/III pyramidal cells in rat barrel cortex. Neuron. 2000; 27:45–56. [PubMed: 10939330]

Feldman DE, Brecht M. Map plasticity in somatosensory cortex. Science. 2005; 310:810–815. [PubMed: 16272113]

Furuta T, Kaneko T, Deschênes M. Septal neurons in barrel cortex derive their receptive field input from the lemniscal pathway. J Neurosci. 2009; 29:4089–4095. [PubMed: 19339604]

Hartman BK, Agrawal HC, Agrawal D, Kalmbach S. Development and maturation of central nervous system myelin: Comparison of immunohistochemical localization of proteolipid protein and basic protein in myelin and oligodendrocytes. Proc Natl Acad Sci USA. 1982; 79:4217–4220. [PubMed: 6180437]

Hess RF, Li X, Mansouri B, Thompson B, Hansen BC. Selectivity as well as sensitivity loss characterizes the cortical spatial frequency deficit in amblyopia. Hum Brain Mapp. 2009; 30:4054–4069. [PubMed: 19507159]

Inan M, Crair MC. Development of cortical maps: Perspectives from the barrel cortex. Neuroscientist. 2007; 13:49–61. [PubMed: 17229975]

Jacobs EC, Campagnoni C, Kampf K, Reyes SD, Kalra V, Handley V, Xie YY, et al. Visualization of corticofugal projections during early cortical development in a tau-GFP-transgenic mouse. Eur J Neurosci. 2007; 25:17–30. [PubMed: 17241263]

Keller A, Carlson GC. Neonatal whisker clipping alters intracortical, but not thalamocortical projections, in rat barrel cortex. J Comp Neurol. 1999; 412:83–94. [PubMed: 10440711]

Keller A, White EL, Cipolloni PB. The identification of thalamocortical axon terminals in barrels of mouse Sml cortex using immunohistochemistry of anterogradely transported lectin (*Phaseolus vulgaris*-leucoagglutinin). Brain Res. 1985; 343:159–165. [PubMed: 4041849]

Kichula EA, Huntley GW. Developmental and comparative aspects of posterior medial thalamocortical innervation of the barrel cortex in mice and rats. J Comp Neurol. 2008; 509:239–258. [PubMed: 18496871]

Landers M, Philip Zeigler H. Development of rodent whisking: Trigeminal input and central pattern generation. Somatosens Mot Res. 2006; 23:1–10. [PubMed: 16846954]

Lu QR, Yuk D, Alberta JA, Zhu Z, Pawlitzky I, Chan J, McMahon AP, et al. Sonic hedgehog--regulated oligodendrocyte lineage genes encoding bHLH proteins in the mammalian central nervous system. Neuron. 2000; 25:317–329. [PubMed: 10719888]

Lu SM, Lin RC. Thalamic afferents of the rat barrel cortex: A light- and electron-microscopic study using *Phaseolus vulgaris* leucoagglutinin as an anterograde tracer. Somatosens Mot Res. 1993; 10:1–16. [PubMed: 8484292]

Mangin JM, Li P, Scafidi J, Gallo V. Experience-dependent regulation of NG2 progenitors in the developing barrel cortex. Nat Neurosci. 2012; 15:1192–1194. [PubMed: 22885848]

Maravall M, Koh IY, Lindquist WB, Svoboda K. Experience dependent changes in basal dendritic branching of layer 2/3 pyramidal neurons during a critical period for developmental plasticity in rat barrel cortex. Cereb Cortex. 2004; 14:655–664. [PubMed: 15054062]

NIH-PA Author Manuscript

NIH-PA Author Manuscript

NIH-PA Author Manuscript

Matthews RT, Kelly GM, Zerillo CA, Gray G, Tiemeyer M, Hockfield S. Aggrecan glycoforms contribute to the molecular heterogeneity of perineuronal nets. J Neurosci. 2002; 22:7536–7547. [PubMed: 12196577]

McNally KR, Peters A. A new method for intense staining of myelin. J Histochem Cytochem. 1998; 46:541–545. [PubMed: 9575041]

McRae PA, Rocco MM, Kelly G, Brumberg JC, Matthews RT. Sensory deprivation alters aggrecan and perineuronal net expression in the mouse barrel cortex. J Neurosci. 2007; 27:5405–5413. [PubMed: 17507562]

Micheva KD, Beaulieu C. Quantitative aspects of synaptogenesis in the rat barrel field cortex with special reference to GABA circuitry. J Comp Neurol. 1996; 373:340–354. [PubMed: 8889932]

Morishita H, Hensch TK. Critical period revisited: Impact on vision. Curr Opin Neurobiol. 2008; 18:101–107. [PubMed: 18534841]

Norton WT, Poduslo SE. Myelination in rat brain: Changes in myelin composition during brain maturation. J Neurochem. 1973; 21:759–773. [PubMed: 4754856]

Oberlaender M, Ramirez A, Bruno RM. Sensory experience restructures thalamocortical axons during adulthood. Neuron. 2012; 74:648–655. [PubMed: 22632723]

Pesavento MJ, Rittenhouse CD, Pinto DJ. Response sensitivity of barrel neuron subpopulations to simulated thalamic input. J Neurophysiol. 2010; 103:3001–3016. [PubMed: 20375248]

Pinto DJ, Brumberg JC, Simons DJ. Circuit dynamics and coding strategies in rodent somatosensory cortex. J Neurophysiol. 2000; 83:1158–1166. [PubMed: 10712446]

Pizzorusso T, Medini P, Berardi N, Chierzi S, Fawcett JW, Maffei L. Reactivation of ocular dominance plasticity in the adult visual cortex. Science. 2002; 298:1248–1251. [PubMed: 12424383]

Salami M, Itami C, Tsumoto T, Kimura F. Change of conduction velocity by regional myelination yields constant latency irrespective of distance between thalamus and cortex. Proc Natl Acad Sci USA. 2003; 100:6174–6179. [PubMed: 12719546]

Seelke AM, Dooley JC, Krubitzer LA. The emergence of somatotopic maps of the body in S1 in rats: The correspondence between functional and anatomical organization. PLoS One. 2012; 7:e32322. [PubMed: 22393398]

Shoykhet M, Simons DJ. Development of thalamocortical response transformations in the rat whisker-barrel system. J Neurophysiol. 2008; 99:356–366. [PubMed: 17989240]

Simons DJ, Durham D, Woolsey TA. Functional organization of mouse and rat SmI barrel cortex following vibrissal damage on different postnatal days. Somatosens Res. 1984; 1:207–245. [PubMed: 6494665]

Simons DJ, Land PW. Early experience of tactile stimulation influences organization of somatic sensory cortex. Nature. 1987; 326:694–697. [PubMed: 3561512]

Soazo M, Garcia GB. Vanadium exposure through lactation produces behavioral alterations and CNS myelin deficit in neonatal rats. Neurotoxicol Teratol. 2007; 29:403–510.

Sun QQ. Experience-dependent intrinsic plasticity in interneurons of barrel cortex layer IV. J Neurophysiol. 2009; 102:2955–2973. [PubMed: 19741102]

Thompson AM, Bannister PA. Interlaminar connections in the neocortex. Cortex. 2003; 13:5–14.

Toda T, Hayakawa I, Matsubayahi Y, Tanaka K, Ikenka K, Lu QR, Kawasaki H. Termination of lesion-induced plasticity in the mouse barrel cortex in the absence of oligodendrocytes. Mol Cell Neurosci. 2008; 39:40–49. [PubMed: 18588982]

Van der Loos H, Woolsey TA. Somatosensory cortex: Structural alterations following early injury to sense organs. Science. 1973; 179:395–398. [PubMed: 4682966]

Vincze A, Mazlo M, Seress L, Komoly S, Abraham H. A correlative light and electron microscopic study of postnatal myelination in the murine corpus callosum. Int J Dev Neurosci. 2008; 26:575–584. [PubMed: 18556167]

Wahlsten D, Colbourne F, Pleas R. A robust, efficient and flexible method for staining myelinated axons in blocks of brain tissue. J Neurosci Methods. 2003; 123:207–214. [PubMed: 12606069]

Waite PM. Normal nerve fibers in the barrel region of developing and adult mouse cortex. J Comp Neurol. 1977; 173:165–174. [PubMed: 845281]

NIH-PA Author Manuscript

NIH-PA Author Manuscript

NIH-PA Author Manuscript

Wells MA, Dittmer JC. A comprehensive study of the postnatal changes in concentration of the lipids developing rat brain. Biochemistry. 1967; 6:3169–3175. [PubMed: 6056982]

Wilbrect L, Holman A, Wright N, Fox K, Svoboda K. Structural plasticity underlies experience-dependent functional plasticity of cortical circuits. J Neurosci. 2010; 30:4927–4932. [PubMed: 20371813]

Wimmer VC, Browser PJ, Kenner T, Bruno RM. Experience-induced plasticity of thalamocortical axons in both juveniles and adults. J Comp Neurol. 2010; 518:4629–4648. [PubMed: 20886626]

Woolsey TA, Van der Loos H. The structural organization of layer IV in the somatosensory region (S1) of mouse cerebral cortex. Brain Res. 1970; 17:205–242. [PubMed: 4904874]

Yamazaki Y, Hokum Y, Kaneko K, Fuji S, Got K, Kato H. Oligodendrocytes: Facilitating axonal conduction by more than myelination. Neuroscientist. 2010; 16:11–18. [PubMed: 19429890]

Zhou Q, Wang S, Anderson DJ. Identification of a novel family of oligodendrocyte lineage-specific basic helix-loop-helix transcription factors. Neuron. 2000; 25:331–343. [PubMed: 10719889]

Zuo Y, Yang G, Kwon E, Gann WB. Long-term sensory deprivation prevents dendritic spine loss in primary somatosensory cortex. Nature. 2005; 436:261–265. [PubMed: 16015331]

NIH-PA Author Manuscript
NIH-PA Author Manuscript
NIH-PA Author Manuscript

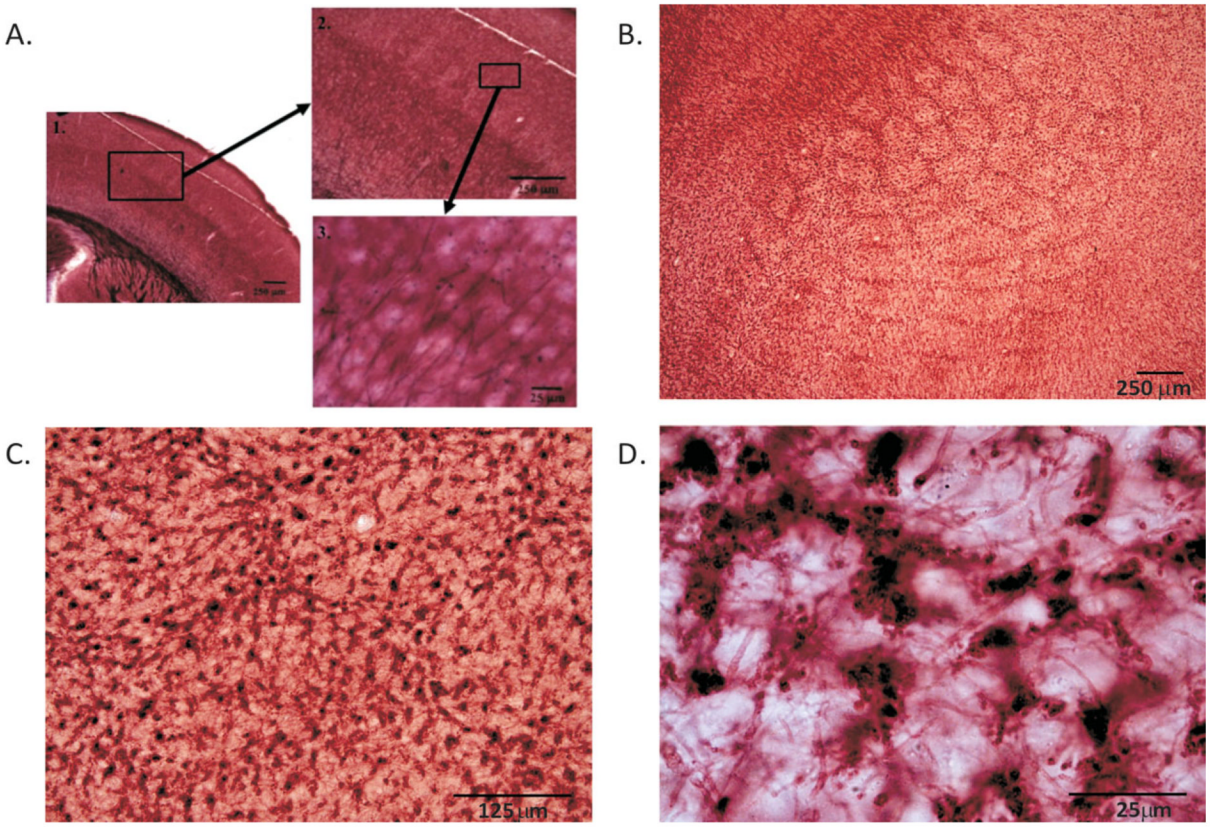

Figure 1.
P60 control tissue stained for myelin. Coronal section reveals myelinated axons in the barrel cortex running perpendicular to the pial surface terminating by layer IV (A). Low-magnification images reveal the barrel pattern (B), whereas higher magnifications (C and D) highlight individual myelinated axons cut in cross section in the tangential plane. Note that myelinated axons are sparser within the barrel hollows than in the septa/wall regions.

NIH-PA Author Manuscript
NIH-PA Author Manuscript
NIH-PA Author Manuscript

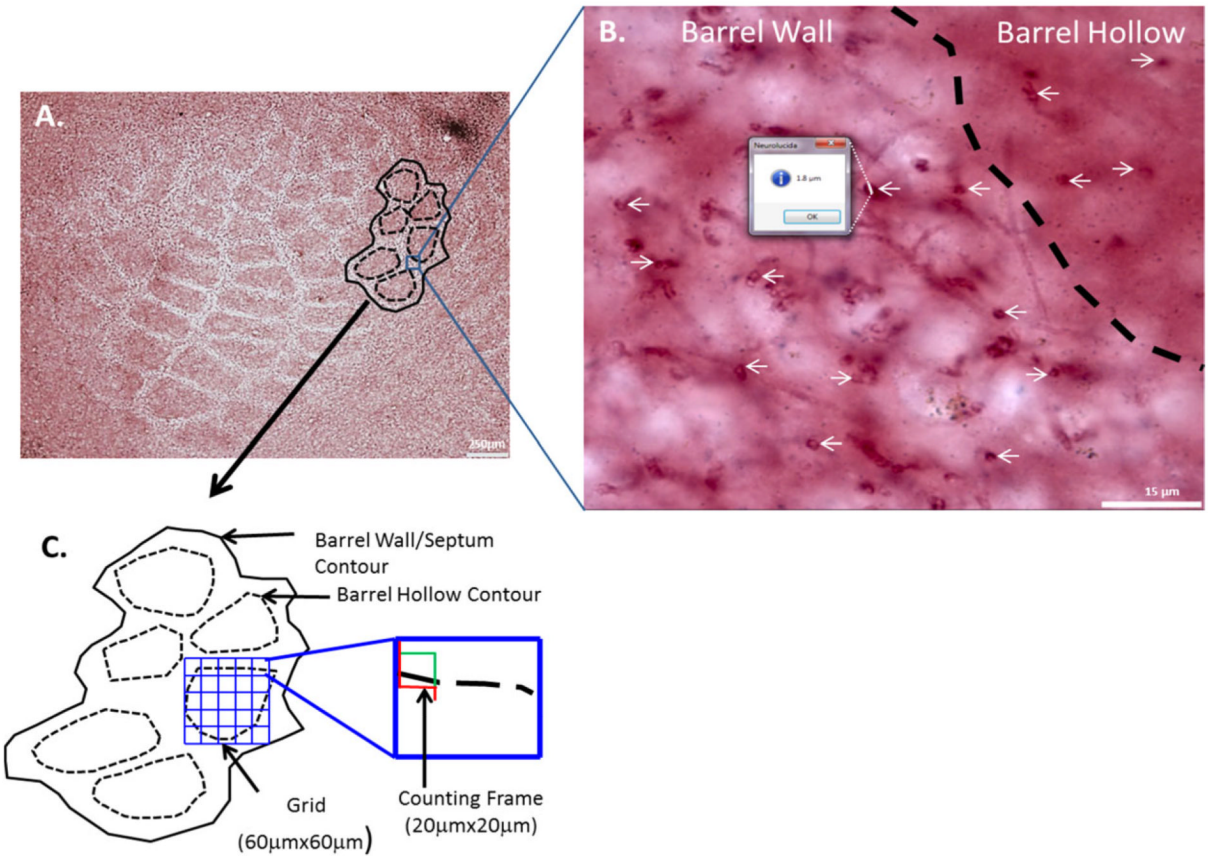

Figure 2.

Quantifying myelin. A P60 AuCl-stained tangential section (A) with barrel wall and barrel hollow contours indicated. High magnification (B) displays the difference in axon density between barrel wall and hollow (B) and how the quick measure line tool was used to quantify axon diameter. A schematic of the contours and counting frames that were utilized for stereological analyses is depicted (C). The counting frame (red and green box) is placed by the software program (Stereo Investigator) in the top left corner of the grid (blue lines), myelinated axons that cross the green line are counted those that intersect the red line are not to prevent double counting. [Color figure can be viewed in the online issue, which is available at wileyonlinelibrary.com.]

NIH-PA Author Manuscript

NIH-PA Author Manuscript

NIH-PA Author Manuscript

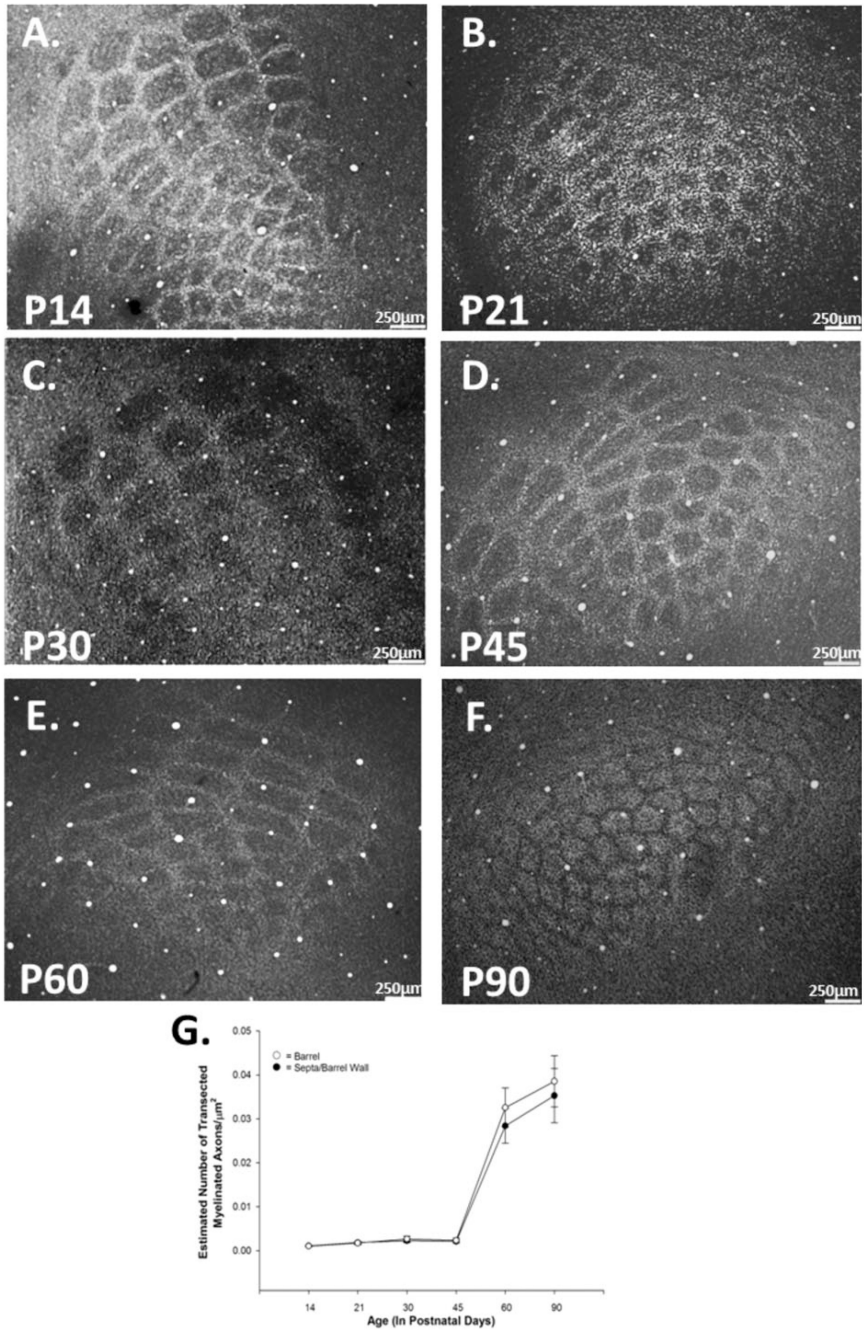

Figure 3.

Density of myelinated axons increases significantly during development. Control tissue stained for myelin at P14 (A), P21 (B), P30 (C), P45 (D), P60 (E), and P90 (F). Myelination increases over normal development in both the barrel hollow and septal/barrel wall regions. Quantification of myelinated axonal density (G) reveals a significant increase between P45 and P60 in the barrel [$F(5,26) = 22.304$, $p < 0.001$] and in the septa [$F(5,26) = 28.616$, $p < 0.001$]. Data points represent population means and one standard error of the mean.

NIH-PA Author Manuscript

NIH-PA Author Manuscript

NIH-PA Author Manuscript

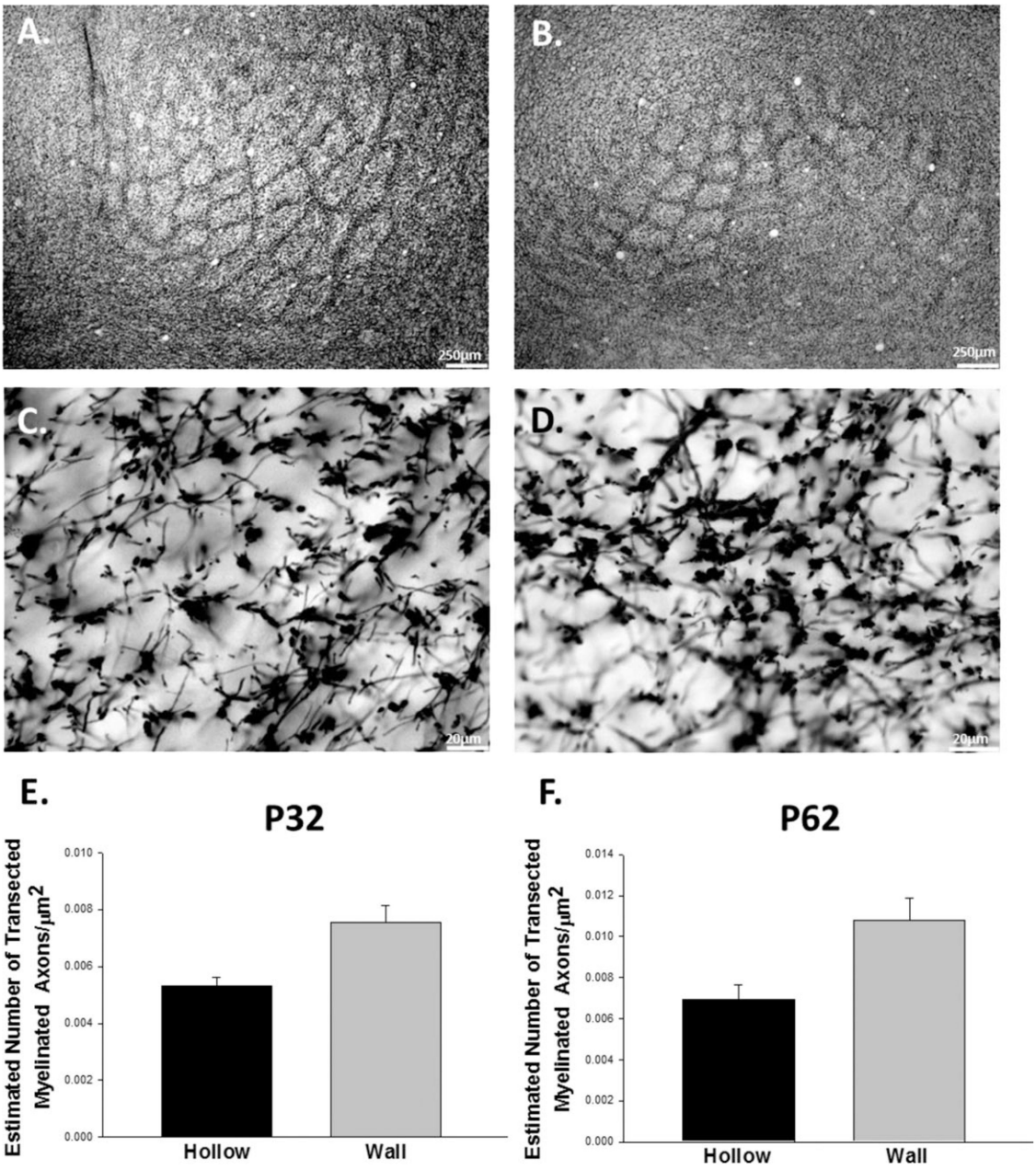

Figure 4.

Myelin basic protein staining in the mouse barrel cortex. Tangential sections at P32 tangential sections at low (A) and high magnifications (C) reveal a barrel pattern as do images from P62 animals at low (B) and high magnifications (D). Quantification of myelin basic protein + axons in the barrel hollow and barrel wall shows that barrel walls have greater densities of transected myelinated axons than barrel hollows at both time points (E and F).

NIH-PA Author Manuscript
NIH-PA Author Manuscript
NIH-PA Author Manuscript

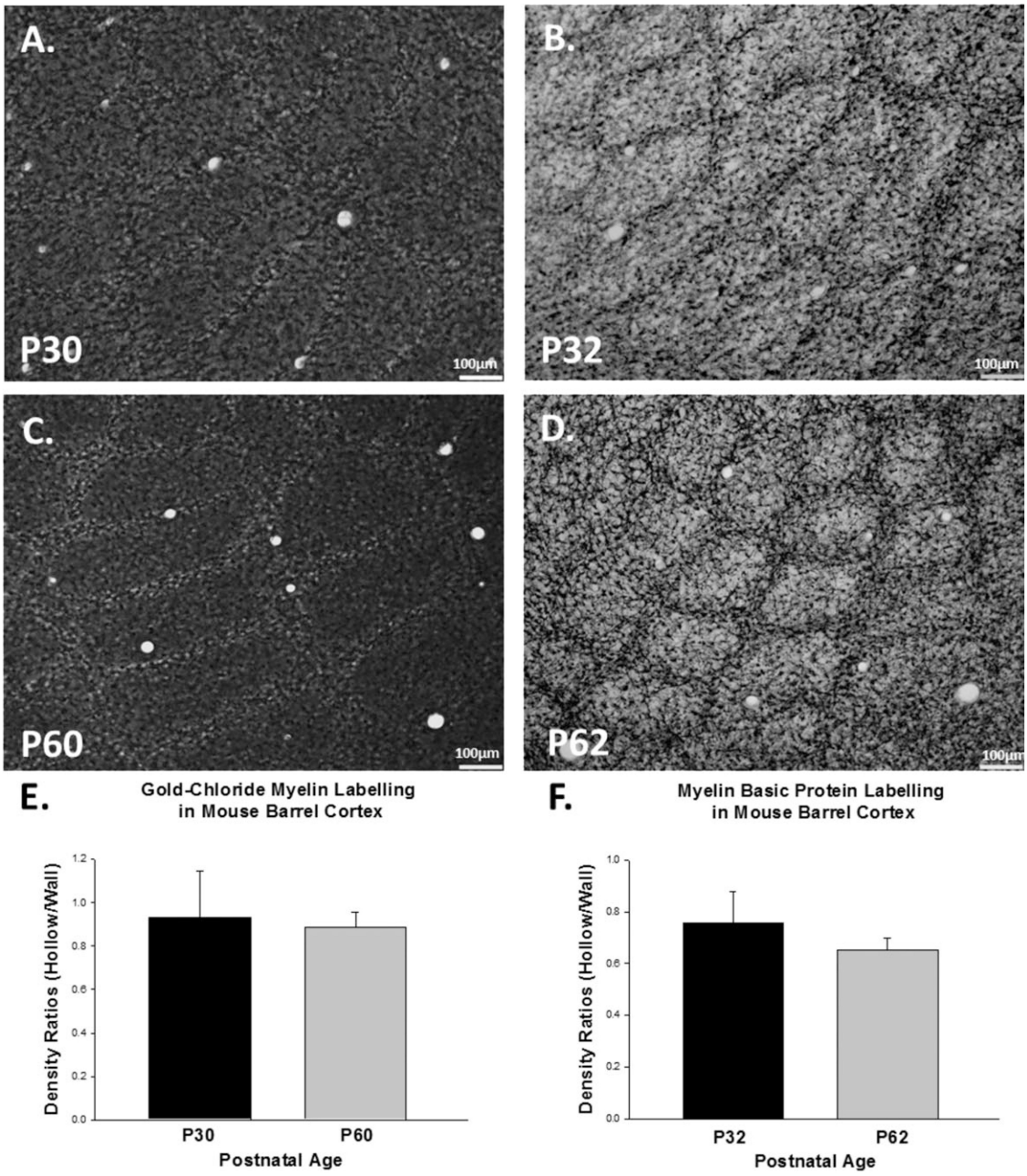

Figure 5.

Gold chloride labeling and myelin basic protein labeling are equivalent in the mouse barrel cortex. P30 and P60 tangential sections using AuCl labeling (A and C) revealed similar patterns of staining when compared P32 and P62 tangential sections labeled with an antibody to myelin basic protein (B and D). The ratio of barrel hollow to barrel wall is consistent between AuCl (E) and myelin basic protein labeling (F).

NIH-PA Author Manuscript

NIH-PA Author Manuscript

NIH-PA Author Manuscript

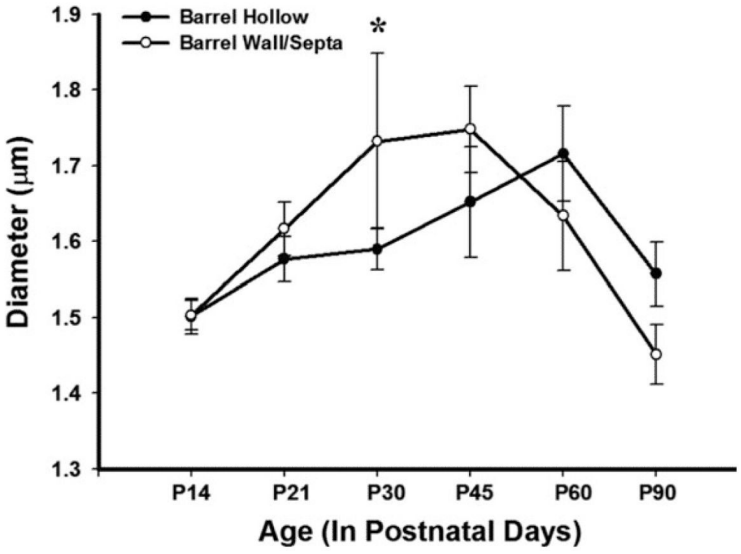

Figure 6.

Diameter of myelinated axons increases significantly during development. Myelin diameter significantly increased over development in both the barrel hollow and barrel wall/septal regions peaking at P45–P60 before returning to mature levels at P90 [$F(13,766) = 14.685$, $p < 0.001$; $F(13,766) = 18.778$, $p < 0.001$, respectively]. The data represent population means and one standard error of the mean.

NIH-PA Author Manuscript
NIH-PA Author Manuscript
NIH-PA Author Manuscript

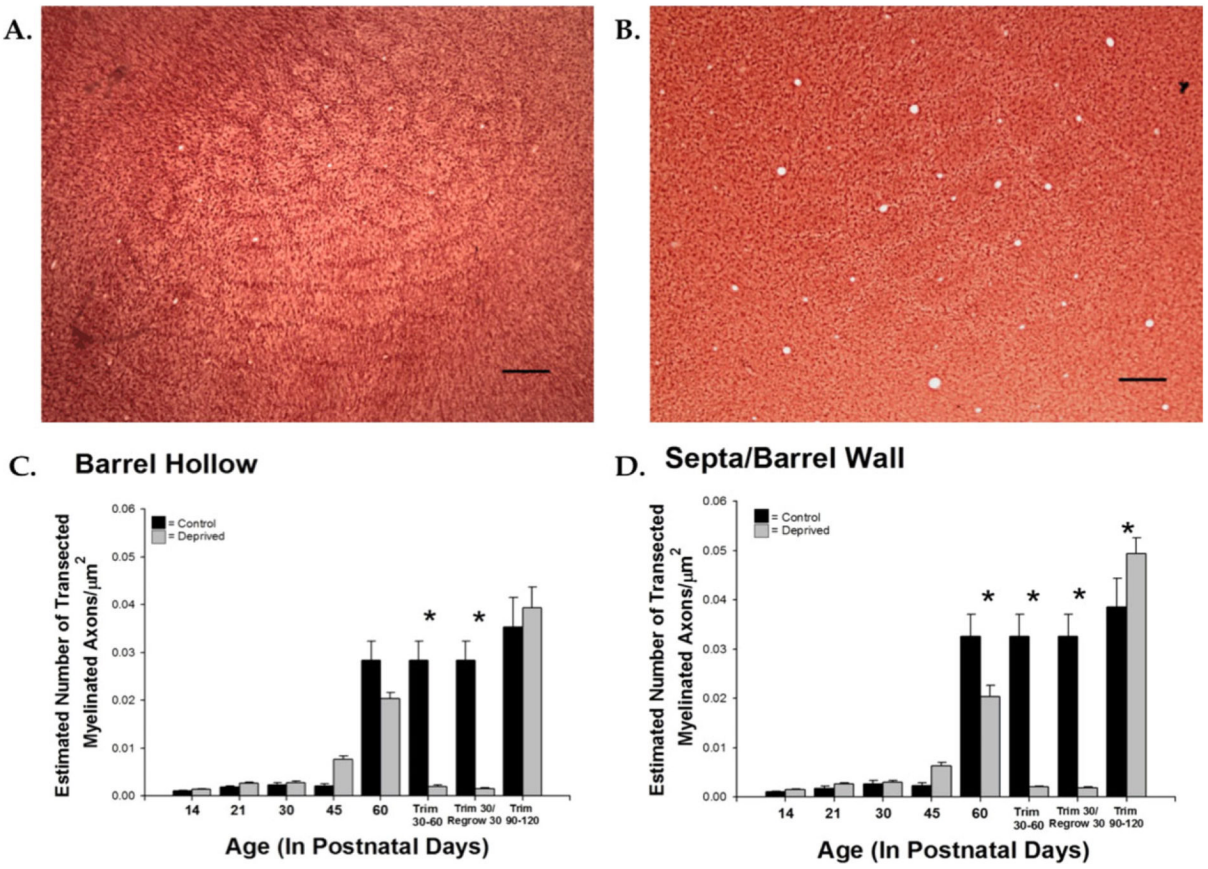

Figure 7.

Whisker trimming decreases density of myelinated axons in the barrel and septal/barrel wall regions. Control (A) and deprived (B) tissue at P60 stained for myelin. Myelination is significantly reduced in the barrel hollow region of the sensory-deprived animals in the P30-P60 trim group and in the Trim30/Regrow30 group [$F(13,64) = 36.369$, $p < 0.001$] (C). Myelination is significantly reduced in the septal/barrel wall region of sensory-deprived animals at P60, and in the P30-P60 trim group, Trim30/Regrow30 group, and an increase in the P90-P120 trim group [$F(13,64) = 51.015$, $p < 0.001$] (D). Bars represent population means and one standard error of the mean. [Color figure can be viewed in the online issue, which is available at wileyonlinelibrary.com.]

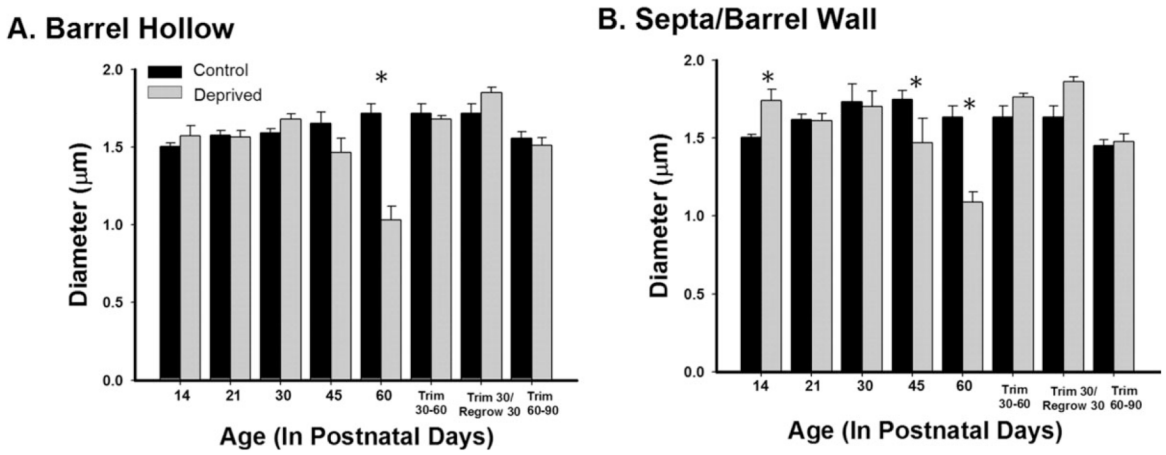

Figure 8.

Whisker trimming decreases the diameter of transected myelinated axons. Whisker trimming decreased the diameter of transected myelinated axons in the barrel hollow (A) at P60 [$F(14,765) = 13.693$, $p < 0.001$] and in the septa/barrel wall (B) at P45 and P60 [$F(13,766) = 18.778$, $p < 0.001$]. Bars represent population means and one standard error of the mean.

NIH-PA Author Manuscript NIH-PA Author Manuscript NIH-PA Author Manuscript

NIH-PA Author Manuscript
NIH-PA Author Manuscript
NIH-PA Author Manuscript

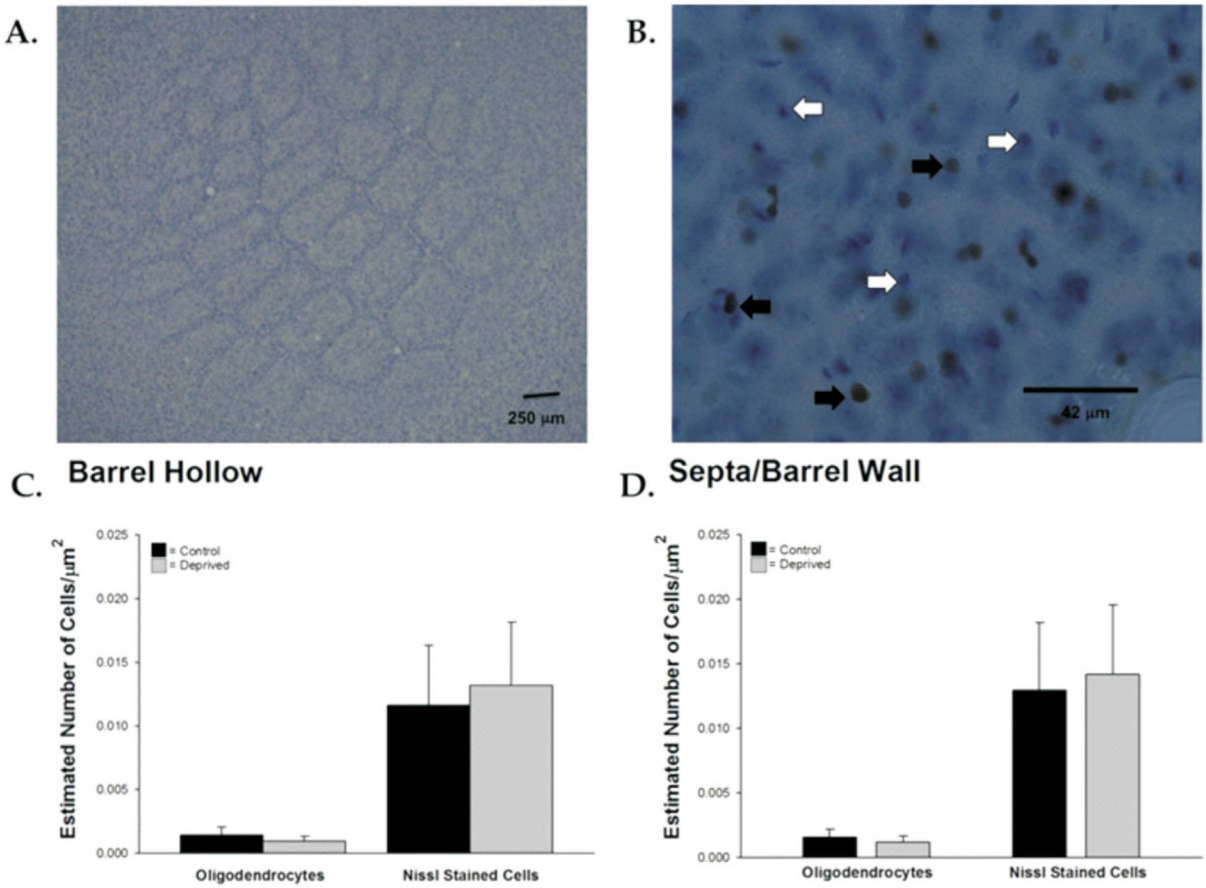

Figure 9.

Cell density and oligodendrocyte density were not affected by sensory deprivation. Representative nissl-stained tangential section from P60 control animal at low magnification (A) shows the barrel field and Olig2+ oligodendrocytes. White arrows indicate nissl-stained cells, and black arrows indicate cells double stained for both Olig2+ and nissl. Overall cell numbers and oligodendrocyte density were unaffected by sensory deprivation (C and D). Bars represent population means and one standard error of the mean. [Color figure can be viewed in the online issue, which is available at wileyonlinelibrary.com.]

NIH-PA Author Manuscript

NIH-PA Author Manuscript

NIH-PA Author Manuscript

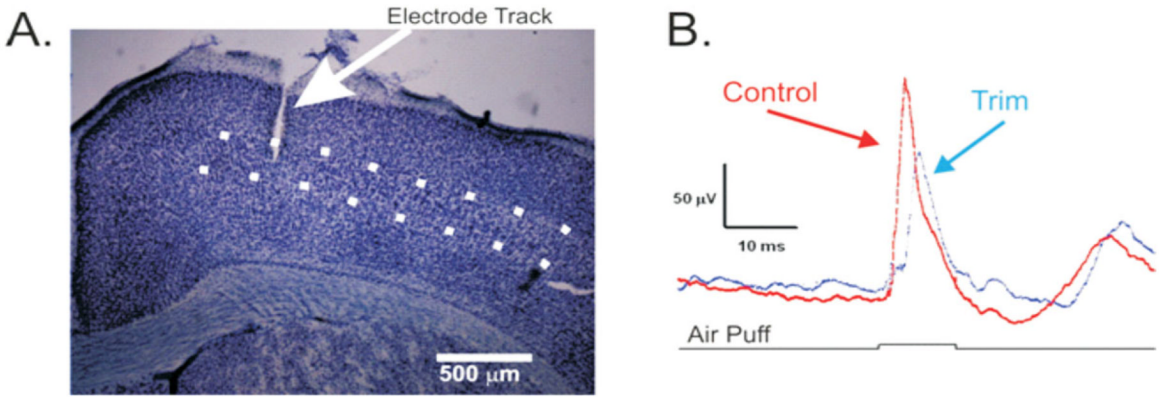

Figure 10.

Local field potential recordings from barrel cortex. Tungsten microelectrodes were manually inserted into layer IV (dotted lines, A). Local field potentials reveal that responses from the intact side (control, red trace) had a faster rate of rise than those on the deprived side (trim, blue trace). Black trace indicates onset and offset of the air puff, and field potentials are averaged in response to 100 stimulus presentations. [Color figure can be viewed in the online issue, which is available at wileyonlinelibrary.com.]

NIH-PA Author Manuscript

NIH-PA Author Manuscript

NIH-PA Author Manuscript

Table 1
Estimated Density of Myelinated Axons

	Barrel Wall/Septa			Barrel Hollow		
	n	Mean (Axons/10 μm^2)	SD	*n*	Mean (Axons/10 μm^2)	SD
P14 Control	6	0.107	0.023	6	0.106	0.037
P14 Deprived	5	0.139	0.041	5	0.146	0.042
P21 Control	6	0.185	0.073	6	0.175	0.101
P21 Deprived	6	0.262	0.068	6	0.262	0.052
P30 Control	4	0.228	0.097	4	0.268	0.130
P30 Deprived	6	0.275	0.079	6	0.306	0.079
P45 Control	5	0.213	0.083	5	0.235	0.119
P45 Deprived	8	0.767	0.206	8	0.635	0.183
P60 Control	5	2.841	0.886	5	3.258	0.993
P60 Deprived	6	2.038	0.303	6	2.036	0.571
P60 Regrow	5	0.193	0.089	5	0.204	0.048
P60 Adult Trim 30–60	5	0.157	0.046	5	0.188	0.051
P90 Control	6	3.212	1.462	6	3.549	1.381
P90 Adult Trim 60–90	5	4.204	0.942	5	5.189	0.782

n reflects the number of animals in each group.

NIH-PA Author Manuscript NIH-PA Author Manuscript NIH-PA Author Manuscript

Table 2

Bonferroni-Adjusted Pairwise Comparisons for Barrel Hollow and Septal/Barrel Wall for Myelinated Axon Density

	P14C	P14D	P21C	P21D	P30C	P30D	P45C	P45D	P60C	P60D	P60R	P60A1	P90C	P90A2
P14C		*NS*	*NS*	*NS*	*NS*	*NS*	*NS*	*NS*	**	**	*NS*	*NS*	**	**
P14D	NS		*NS*	*NS*	*NS*	*NS*	*NS*	*NS*	**	**	*NS*	*NS*	**	**
P21C	NS	NS		*NS*	*NS*	*NS*	*NS*	*NS*	**	**	*NS*	*NS*	**	**
P21D	NS	NS	NS		*NS*	*NS*	*NS*	*NS*	**	**	*NS*	*NS*	**	**
P30C	NS	NS	NS	NS		*NS*	*NS*	*NS*	**	**	*NS*	*NS*	**	**
P30D	NS	NS	NS	NS	NS		*NS*	*NS*	**	**	*NS*	*NS*	**	**
P45C	NS	NS	NS	NS	NS	NS		*NS*	**	**	*NS*	*NS*	**	**
P45D	NS	NS	NS	NS	NS	NS	NS		**	**	*NS*	*NS*	**	**
P60C	**	**	**	**	**	**	**	*		**	**	**	*NS*	**
P60D	**	**	**	**	**	**	**	**	NS		**	**	**	**
P60R	NS	NS	NS	NS	NS	NS	NS	NS	**	**		*NS*	**	**
P60A1	NS	NS	NS	NS	NS	NS	NS	NS	**	**	NS		**	**
P90C	**	**	**	**	**	**	**	**	NS	**	**	**		**
P90A2	**	**	**	**	**	**	**	**	**	**	**	**	NS	

P, postnatal day; C, control group; D, sensory-deprived group; R, Trim Regrow (30-day trim, 30-day regrow); A1, adult Trim 30–60; A2, adult Trim 60–90; NS, nonsignificant; italicized text, barrel hollow data; nonitalicized text, septal/barrel wall data.

* $p < 0.05$

** $p < 0.01$.

NIH-PA Author Manuscript

NIH-PA Author Manuscript

NIH-PA Author Manuscript

Table 3

Diameters of Myelinated Axons

	Barrel Wall/Septa			Barrel Hollow		
	n	**Mean (μm)**	**SD**	***n***	**Mean (μm)**	**SD**
P14 Control	60	1.50	0.15	60	1.50	0.16
P14 Deprived	50	1.57	0.20	50	1.74	0.22
P21 Control	60	1.57	0.26	60	1.61	0.25
P21 Deprived	60	1.56	0.27	60	1.61	0.27
P30 Control	40	1.59	0.27	40	1.73	0.34
P30 Deprived	60	1.67	0.30	60	1.70	0.38
P45 Control	60	1.56	0.33	60	1.65	0.35
P45 Deprived	80	1.46	0.41	80	1.40	0.46
P60 Control	40	1.73	0.35	40	1.69	0.36
P60 Deprived	50	1.12	0.32	50	1.13	0.25
P60 Regrow	50	1.85	0.23	50	1.86	0.21
P60 Adult	50	1.67	0.15	50	1.76	0.02
Trim 30–60						
P90 Control	70	1.55	0.35	70	1.45	0.32
P90 Adult	50	1.51	0.36	50	1.47	0.35
Trim 60–90						

n reflects the number of axons quantified (~ 10 axons per animal).

NIH-PA Author Manuscript NIH-PA Author Manuscript NIH-PA Author Manuscript

Table 4

Bonferroni *Post Hoc* Pairwise Comparisons for Barrel Hollow and Septal/Barrel Wall for Myelinated Axonal Diameter

	P14C	P14D	P21C	P21D	P30C	P30D	P45C	P45D	P60C	P60D	P60R	P60A1	P90C	P90A2
P14C		*NS*	*NS*	*NS*	*NS*	*NS*	*NS*	*NS*	*NS*	**	**	*NS*	*NS*	*NS*
P14D	**		*NS*	*NS*	*NS*	*NS*	*NS*	*NS*	*NS*	**	**	*NS*	*NS*	*NS*
P21C	NS	NS		*NS*	*NS*	*NS*	*NS*	*NS*	*NS*	**	**	*NS*	*NS*	*NS*
P21D	NS	NS	NS		*NS*	*NS*	*NS*	*NS*	*NS*	**	**	*NS*	*NS*	*NS*
P30C	*	NS	NS	NS		*NS*	*NS*	*NS*	*NS*	**	**	*NS*	*NS*	*NS*
P30D	NS	NS	NS	NS	NS		*NS*	**	*NS*	**	*NS*	*NS*	*NS*	*NS*
P45C	NS	NS	NS	NS	NS	NS		*NS*	*NS*	**	**	*NS*	*NS*	*NS*
P45D	NS	**	**	*	**	**	**		**	**	**	**	*NS*	*NS*
P60C	NS	NS	NS	NS	NS	NS	NS	*		**	*NS*	*NS*	*NS*	*
P60D	**	**	**	**	**	**	**	**	**		**	**	*NS*	**
P60R	**	NS	**	**	NS	NS	*	**	NS	**		*NS*	**	**
P60A1	**	NS	NS	NS	NS	NS	*	**	NS	**	**		*NS*	*NS*
P90C	NS	**	NS	NS	**	**	*	NS	*	**	**	**		*NS*
P90A2	NS	**	NS	NS	*	*	NS	NS	NS	**	**	**	NS	

P, postnatal day; C, control group; D, sensory-deprived group; R, Trim Regrow (30-day trim, 30-day regrow); A1, adult Trim 30–60; A2, adult Trim 60–90; NS, nonsignificant; italicized text, barrel hollow data; nonitalicized text, septal/barrel wall data.

* $p < 0.05$

** $p < 0.01$.